# Patterns, drivers and implications of ascidian distributions in a rapidly deglaciating fjord, King George Island, West Antarctic Peninsula

Dong-U Kim [a,b,1], Jong Seong Khim [b,2], In-Young Ahn [a,*,3]

[a] *Division of Ocean Sciences, Korea Polar Research Institute (KOPRI), Incheon 21990, Republic of Korea*
[b] *School of Earth and Environmental Sciences & Research Institute of Oceanography, Seoul National University, Seoul 08826, Republic of Korea*

### ABSTRACT

We report strong evidence for the utility of ascidian communities as sentinel organisms for monitoring nearshore Antarctic marine ecosystem response to climate-induced warming and glacial melting. Ascidians are one of the most common Antarctic epibenthic megafauna, but information on their distribution and the determinants is still scarce. In this study we investigated spatial patterns of ascidians in Marian Cove (MC), a rapidly deglaciating fjord in the West Antarctic Peninsula, one of the most rapidly warming regions on earth. We also analyzed key drivers structuring the communities and assessed their relevance to glacial retreat and following processes. The first applied ROV survey in MC discovered that ascidians were the most diverse (14 out of 64 taxa) taxa with the greatest abundance ($\sim$264 inds·m$^{-2}$). Ascidian abundance and diversity greatly varied in space, by distance from glacier and/or depths, explaining $\sim$64% of total megafaunal variations. Notably, in deep seabed (50–90 m) they shifted distinctly from early colonization communities near glacier (0.2 km to glacier) with predominance of two opportunistic species, *Molgula pedunculata* and *Cnemidocarpa verrucosa*, to mature communities at the most remote site (3.5 km). A set of analyses revealed that such shifts were related mostly to changes in sediment properties that develop in association with glacial retreat and consequent processes. Sediment composition, grain size and sorting collectively explained outward increasing physical stability apparently with decreased influence of glacial retreat, supporting ascidian community maturing at the deep and distant site. BIOENV analysis indicated that "distance" to glacier is one key factor influencing ascidian community structure in the deep seabed. Overall, the results of the analyses strongly indicated that physical disturbances (mainly sedimentation and ice scouring) accompanying glacial retreat are an important force shaping ascidian assemblages in the cove, and that these forces are altered by the distance from the glacier and water depth. Notably, in this fjord, the period of sea bed deglaciation was roughly proportional to the distance to glacier over the last six decades. This suggested that the ascidian shift identified in this study reflects a long-term successional process associated with glacial retreat in the past in MC, which in turn warrants to project future changes in this glacial fjord and possibly other similar environments.

## 1. Introduction

The West Antarctic Peninsula (WAP) has warmed significantly over the last half century and, consequently, both marine-terminating and land glaciers have been rapidly shrinking (Cook et al., 2014; Rignot et al., 2019). In particular, marine-terminating glacial retreat, which is accompanied by a variety of processes, including ice scouring and inflow of sediment-laden meltwater, appears to exert a profound influence on coastal marine ecosystems by altering habitat environments, and eventually impacting inhabitants (Smale and Barnes, 2008). Slow-moving or

**Fig. 1.** (a) Map showing the locations of King George Island, Maxwell Bay, and its tributary embayments including Marian Cove (MC). (b) Bathymetry of MC. The bathymetric contours were constructed from data obtained through a seismic survey (Shin et al., 2012). The area in white represents glacier or snow cover. (c) ROV survey and sampling stations (MC2, MC3, MC4, and MC5) in orange squares and glacial retreat lines over six decades. Glacial retreat lines were drawn based on information obtained from satellite images and aerial photographs (updated from Moon et al., 2015). (For interpretation of the references to color in this figure legend, the reader is referred to the web version of this article.)

sedentary benthic communities in shallow nearshore areas are most vulnerable to these processes with their species richness and diversity strongly impacted (Siciński et al., 2012; Moon et al., 2015; Sahade et al., 2015). On the other hand, some opportunistic species colonize rapidly newly exposed habitats after glacial retreat (Peck et al., 2010; Quartino et al., 2013; Lagger et al., 2018). Thus, biological response to glacial retreat is highly species-specific, which complicates assessment of the overall ecosystem response. Therefore, selection of sentinel organisms that can be used to assess reliably the responses of benthic communities to glacial retreat and to predict future shifts in overall benthic communities is of critical concern.

Ascidians are among the most common benthic fauna in the Antarctic, with a broad distribution from shallow to deep waters (Primo and Vazquez, 2014; Segelken-Voigt et al., 2016). In particular, they have been found to occur at high densities around the South Shetland archipelago, including King George Island (KGI) (Sahade et al., 1998; Tatiàn et al., 1998; Lagger et al., 2018). They colonize rapidly through fast growth and reproduction in areas that are newly exposed after glacial retreat (Teixidó et al., 2004; Sahade et al., 2015; Lagger et al., 2017). Some ascidian species act as foundation species by stabilizing habitat for other species or providing substrates for their juveniles as well as other species (Lagger et al., 2018). Ascidians are also one of the dominant sessile suspension feeders in Antarctic epibenthic megafaunal communities (Gili et al., 2006), and they appear to act as an important mediator of energy transfer between the pelagic and benthic ecosystems (Gili et al., 2001). Together, these characteristics make ascidians excellent organisms for monitoring changes in Antarctic benthic ecosystems. Nonetheless, their distribution and its determinants have rarely been studied particularly in relation to climate-induced processes such as glacial retreat.

Marian Cove (MC) is a rapidly warming and deglaciating fjord in the WAP, where tidewater glaciers have retreated approximately 1.9 km over the last six decades (Fig. 1). Benthic faunal assemblages in MC well represent those in shallow Antarctic waters with dominant occurrence (~60%) of suspension feeders, such as ascidians, bryozoans and demosponges (Moon et al., 2015). Moon et al. also demonstrated that glacial retreats have altered habitat properties and consequently impacted the species number and functional diversity of megabenthic communities in the area adjacent to glacier front, and suggested that MC could serve as a model ecosystem for climate-related studies. Further studies on the megabenthic communities in the cove revealed a unique and highly efficient trophic structure based on benthic diatom blooms in association with a variety of filter feeders, including ascidians, sponges and polychaetes (Ahn et al., 2016; Ha et al., 2019). Thus, the previous studies strongly suggested that ascidian communities in this fjord play a key role in terms of both structural and functional aspect. However, quantitative data on ascidian spatial patterns, particularly those on their abundance are scarce, which warrants further studies into their spatial patterns and the determinants as well as their relevance to glacial retreat. Moreover, those previous studies have been conducted only at shallow waters (<35 m) and little is known for benthic communities at deeper waters (a maximum depth of 130 m).

The objectives of this study are to characterize the spatial patterns of ascidians in MC and to identify key drivers structuring the communities, and furthermore to assess their relevance to glacial retreat, with the aim of facilitating their use and enhancing their value for climate-related studies. We used a remotely operated vehicle (ROV) for the first time in MC at depths that were not reachable by SCUBA diving surveys in previous studies. Using the ROV survey, we obtained quantitative images of benthic communities at several sites at varying distance from the glacier front across almost the entire water depth profile.

## 2. Materials and methods

### 2.1. Study area

Marian Cove, where King Sejong Station (62° 13′ S, 58° 46′ W) is located, is a small and confined fjord-like embayment (~4.5 km long and ~1.5 km wide, ~130 m deep) within Maxwell Bay at KGI. KGI is the largest island of the South Shetland Islands, which are located off the northern tip of the WAP (Fig. 1). KGI has a relatively mild maritime climate, and meteorological data from King Sejong Station over recent decades (1988–2018) show an average annual air temperature of −1.8 °C (min = −5.7 °C in July, max = 1.9 °C in January), and generally >0 °C from December through March (Hong et al., 2019).

Seawater temperature in MC varies seasonally from a maximum of ca. 1.5 °C in February to a minimum of ca. −1.8 °C in August (see the Section 2.5). Salinity remains fairly constant from, 33.8 to 34.1 psu, throughout the year, with the tendency to increase slightly toward the bottom (see the Section 2.5). Water circulation appears very limited except during the summer months (Chang et al., 1990), and exchange of water masses with Maxwell Bay is restricted by a shallow sill (~70 m) at the entrance of the cove that bathymetrically separates MC from Maxwell Bay (Yoo et al., 2015). Further information on the hydrographic features of MC during summer has been reported by Yoo et al. (2015).

Tidewater glaciers are well developed in the inner part of MC, and these glaciers have retreated approximately 1.9 km from 1956 to 2017, leaving ~45% of its bottom ice free (Fig. 1). Glacier break-up occurs throughout the summer months (December through March), introducing large volumes of turbid meltwater and icebergs into the cove (Yoon et al., 1998; Ahn et al., 2004; Yoo et al., 2015). A large amount of meltwater is introduced also from the surrounding snowfield throughout the summer months (personal observation). The glaciers in MC are likely to be susceptible to small oscillations in air temperature, as observed at other sites in the northern WAP (Turner et al., 2016; Oliva et al., 2017), corroborating the utility of MC as a site monitoring climate impacts on marine ecosystem in the northern WAP. Notably, glacial retreat in the cove slowed during the cooling period (40 m·yr$^{-1}$, with mean annual temperature of −1.91 °C in 2000–2015), as compared with the preceding warmer period (64 m·yr$^{-1}$ with −1.61 °C in 1989–2000) (see the Section 2.5 for the data acquisition).

### 2.2. ROV survey and sampling

Epibenthic megafaunal assemblages and seabed sediment characteristics were determined from underwater photographs. In-situ images of epibenthic megafauna and substrate types were obtained to depths of 90 m using an ROV (VideoRay Pro4) operated from a rubber boat from December 2017 to February 2018. The ROV was equipped with a video camera (GoPro Hero5), and a stainless steel quadrat (50 × 50 cm) was mounted on the ROV frame to obtain quantitative data on the epifaunal distribution and seabed sediment composition (Fig. S1)

ROV survey stations (MC2, MC3, MC4, and MC5; Fig. 1) were selected based on the previous reports of the level of glacial influence, bottom topography, distance from the glacier terminus, and the time period (in years) of seabed exposure after glacial retreat (Ahn et al., 2004; Moon et al., 2015; Yoo et al., 2015). At each station, the ROV was descended from a boat along the bottom slope in a direction roughly perpendicular to the shoreline, and seabed images within the quadrat frame were taken from each of six water depths (10, 20, 30, 50, 70, and 90 m). The area surveyed by the ROV spanned over 90 m depth and 200 m wide at each station. For obtaining unbiased representative images, images were taken from flat bottom and the distance between the images was kept at least 5 m. Due to differences in slope and bottom topography, total number of images taken (10–22; Table S1) at each depth varied among the stations. Intertidal and shallow (<10 m) subtidal bottom areas that were composed mainly of gravels were excluded

from this study, as they were nearly devoid of large animals.

Ascidian samples were collected by divers and using a dredge from the R/V Araon to aid with species identification in images taken by the ROV. Sediment samples were also collected by divers using a hand-held corer (6.5 cm in diameter, 6 cm in length) (<30 m depths) and from a boat (>30 m depths) with a Van Veen grab (0.05 m$^2$ in surface area, maximum depth of 15 cm) to supplement the seabed substrate information obtained from the ROV images. The sediment samples were also used for analysis of organic matter content as described below.

### 2.3. ROV images and sample analysis

The taxonomic composition and abundance of epibenthic megafauna were determined from images collected by the ROV. All epifaunal animals that were discernable in the images (approximately >1 cm in the longest dimension) were recorded and identified to the lowest taxonomic level possible, using identification descriptions in the literature (Hibberd, 2009; Rauschert and Arntz, 2015; Danis, 2013; Schories and Kohlberg, 2016) and through the database of the World Register of Marine Species (http://www.marinespecies.org) (accessed on May 25, 2020). Small bivalves, gastropods, amphipods and other organisms that occurred mostly as epibionts were not easily discernable in the images and were therefore excluded from analysis. For each image, the percentage of area covered by animals was also determined.

Ascidian taxa were identified to the lowest possible level based on specific morphological characteristics described in the literature (Tatiàn et al., 1998, 2005; Monniot et al., 2011; Alurralde et al., 2013; Schories and Kohlberg, 2016) and also with the aid of ascidian taxonomists (Boon-Jo Rho and Su-Yuan Seo from Natural History Museum, Ewha Womans University, Republic of Korea). Abundance data for each ascidian taxon were then obtained by counting the number within a quadrat frame (50 × 50 cm) and transforming the counted numbers to values per square meter (Table S1). For colonial taxa, each colony was counted as a single individual (Segelken-Voigt et al., 2016).

Linear dimension of each individual was also determined from the ROV-acquired images using ImageJ software (National Institutes of Health, USA). ROV images were taken from above in the water, and body length (L, the longest dimension) of many individuals, particularly those in an upright or standing position could not be determined directly from the images. Therefore, the width (Wd) of each individual was determined, and the measured Wd values were converted to body weight (total wet weight, tww) and L values, using allometric relationships of the three most abundant species (*M. pedunculata*, *C. verrucosa* and *A. challengeri*) (Fig. S2). For the other species, one of the three allometric equations were used based on the similarity of body form. Biomass for each taxon in each quadrat was calculated by summing up the estimated tww of individuals.

Seabed sediment composition was determined from the ROV images as well as the collected sediment samples. Only images with at least 25% bare sediment area (without animals or plants) were used for composition analysis. From these images, the percentages of boulder (>25.5 cm), cobble (6.5–25.5 cm), pebble (6.5–1.0 cm), and smaller sediments (<1 cm) coverage were determined using ImageJ software (Anderson et al., 2007; Smale et al., 2007; Dorschel et al., 2014). Sediment particles smaller than 1 cm in diameter were not distinguishable in the images and were further analyzed using the sediment samples collected by divers and grab sampling. Sediment particles >63 μm were measured with a Ro-Tap® sieve shaker after removal of organic matter using $H_2O_2$, followed by elimination of calcium carbonate with 35% HCl. The finer fractions (<63 μm) were analyzed using a sediment particle size analyzer (Sedigraph® 5120, Micrometrics Inc.).

Total organic carbon (TOC) and total nitrogen (TN) were determined from the surface flocculent layer, which was collected by divers at <30 m and Van Veen grab at >30 m. Sediment samples were freeze-dried and ground, and then total carbon (TC) and TN were analyzed using a Flash 2000 elemental analyzer (Thermo Fisher scientific). TOC was calculated

**Table 1**

Comparison of environmental characteristics among ROV survey stations (MC2, MC3, MC4, and MC5) in Marian Cove. Distances of the stations from the glacier front were determined using the glacier front in the year of 2017 as a baseline (Fig. 1). *The periods of seabed exposure at the stations were estimated based on glacial retreat lines in Fig. 1. **Data were obtained from the long-term monitoring dataset collected at the station (see Section 2.5). ***Sediment composition was determined from quadrat images obtained using an ROV in combination with the results from analysis of sediments collected by divers and grab sampling (refer to Section 2.3 for more details). Mean ± standard deviation values are presented.

| Station | Period of seabed exposure (yr)* | Distance from glacier front (km) | WaterDepth (m) | Water column properties** | | Sediment properties | | | | | | | | |
|---|---|---|---|---|---|---|---|---|---|---|---|---|---|---|
| | | | | AnnualMean temp. (°C) | AnnualMean salinity (psu) | TOC (n = 3) (%) | TN (n = 3) (%) | n | Sediment composition (%)*** | | | | Mean grain size (φ) | Sorting (φ) |
| | | | | | | | | | Gravel | Sand | Silt | Clay | | |
| MC2 | > 62 | 3.5 | 10 | −0.20 | 34.01 | 0.29 ± 0.03 | 0.033 ± 0.008 | 11 | 48.5 ± 21 | 39.5 ± 16 | 4.4 ± 1.8 | 7.6 ± 3.1 | 0.43 ± 1.6 | 7.80 ± 1.4 |
| | | | 20 | −0.25 | 34.04 | 0.60 ± 0.27 | 0.085 ± 0.047 | 5 | 28.8 ± 1.1 | 51.5 ± 0.8 | 12.1 ± 0.2 | 7.7 ± 0.1 | 2.06 ± 0.1 | 6.36 ± 0.1 |
| | | | 30 | −0.28 | 34.06 | 0.59 ± 0.30 | 0.09 ± 0.054 | 7 | 38.9 ± 1.9 | 36.4 ± 1.1 | 15.4 ± 0.5 | 9.4 ± 0.3 | 1.87 ± 0.1 | 6.74 ± 0.1 |
| | | | 50 | −0.35 | 34.09 | 0.69 ± 0.07 | 0.09 ± 0.013 | 14 | 15.7 ± 2.8 | 13.0 ± 0.4 | 42.0 ± 1.4 | 29.3 ± 1.0 | 5.53 ± 0.3 | 4.30 ± 0.3 |
| | | | 70 | −0.42 | 34.11 | 0.58 ± 0.05 | 0.08 ± 0.010 | 10 | 1.5 ± 0.5 | 7.1 ± 0.0 | 56.1 ± 0.3 | 35.3 ± 0.2 | 7.15 ± 0.1 | 2.12 ± 0.1 |
| | | | 90 | −0.47 | 34.13 | 0.61 ± 0.07 | 0.08 ± 0.007 | 15 | 0.7 ± 0.5 | 5.2 ± 0.0 | 54.6 ± 0.3 | 39.4 ± 0.2 | 7.44 ± 0.1 | 1.82 ± 0.1 |
| MC3 | 31–33 | 1.2 | 10 | −0.22 | 33.97 | 0.73 ± 0.03 | 0.116 ± 0.01 | 9 | 58.5 ± 28 | 12.4 ± 8.5 | 18.0 ± 12 | 11.0 ± 7.5 | 0.77 ± 2.7 | 8.01 ± 1.9 |
| | | | 20 | −0.27 | 34.02 | 0.66 ± 0.25 | 0.109 ± 0.04 | 11 | 33.1 ± 27 | 17.1 ± 6.8 | 33.1 ± 13 | 16.7 ± 6.6 | 3.23 ± 2.5 | 6.00 ± 2.0 |
| | | | 30 | −0.29 | 34.04 | 0.66 ± 0.13 | 0.093 ± 0.02 | 10 | 35.9 ± 44 | 9.4 ± 6.6 | 35.1 ± 24 | 19.5 ± 14 | 3.29 ± 4.4 | 5.66 ± 3.4 |
| | | | 50 | −0.32 | 34.07 | 0.32 ± 0.11 | 0.038 ± 0.01 | 13 | 16.2 ± 19 | 24.0 ± 5.6 | 37.7 ± 8.7 | 22.1 ± 5.1 | 4.63 ± 2.0 | 4.70 ± 1.8 |
| | | | 70 | −0.45 | 34.09 | 0.37 ± 0.04 | 0.046 ± 0.01 | 11 | 10.3 ± 5.0 | 11.6 ± 0.6 | 48.2 ± 2.7 | 29.9 ± 1.7 | 5.99 ± 0.6 | 3.66 ± 0.7 |
| | | | 90 | −0.55 | 34.01 | 0.44 ± 0.02 | 0.056 ± 0.004 | 11 | 5.9 ± 6.2 | 8.7 ± 0.6 | 42.0 ± 2.8 | 43.3 ± 2.9 | 6.85 ± 0.7 | 3.00 ± 1.0 |
| MC4 | 17–23 | 0.8 | 10 | −0.26 | 33.97 | 0.43 ± 0.18 | 0.068 ± 0.03 | 12 | 45.5 ± 15 | 32.8 ± 9.0 | 13.0 ± 3.6 | 8.7 ± 2.4 | 1.43 ± 1.3 | 7.12 ± 1.0 |
| | | | 20 | −0.28 | 34.02 | 0.54 ± 0.09 | 0.085 ± 0.03 | 14 | 13.8 ± 4.1 | 31.0 ± 1.5 | 31.0 ± 1.5 | 24.2 ± 1.2 | 4.72 ± 0.4 | 4.63 ± 0.4 |
| | | | 30 | −0.29 | 34.04 | 0.49 ± 0.07 | 0.074 ± 0.008 | 11 | 20.1 ± 0.7 | 29.9 ± 0.3 | 27.0 ± 0.2 | 23.1 ± 0.2 | 4.22 ± 0.1 | 5.12 ± 0.1 |
| | | | 50 | −0.33 | 34.07 | 0.33 ± 0.05 | 0.034 ± 0.005 | 14 | 9.9 ± 4.9 | 16.3 ± 0.9 | 39.9 ± 2.2 | 33.9 ± 1.8 | 5.91 ± 0.5 | 3.83 ± 0.6 |
| | | | 70 | −0.40 | 34.09 | 0.27 ± 0.02 | 0.025 ± 0.002 | 10 | 5.9 ± 7.2 | 10.1 ± 0.8 | 45.2 ± 3.5 | 38.8 ± 3.0 | 6.65 ± 0.7 | 3.01 ± 1.0 |
| | | | 90 | −0.54 | 34.11 | 0.30 ± 0.10 | 0.031 ± 0.008 | 13 | 6.7 ± 2.0 | 12.9 ± 0.3 | 42.7 ± 0.9 | 37.7 ± 0.8 | 6.47 ± 0.2 | 3.31 ± 0.3 |
| MC5 | 7–13 | 0.2 | 10 | −0.27 | 33.99 | 0.45 ± 0.20 | 0.075 ± 0.05 | 13 | 17.8 ± 6.7 | 42.7 ± 3.5 | 26.6 ± 2.2 | 12.8 ± 1.1 | 3.58 ± 0.6 | 5.25 ± 0.6 |
| | | | 20 | −0.27 | 34.03 | 0.53 ± 0.22 | 0.086 ± 0.04 | 19 | 3.0 ± 0.4 | 22.3 ± 0.1 | 50.2 ± 0.2 | 24.5 ± 0.1 | 6.0 ± 0.03 | 2.99 ± 0.1 |
| | | | 30 | −0.28 | 34.05 | 0.46 ± 0.07 | 0.074 ± 0.01 | 16 | 19.0 ± 6.7 | 21.6 ± 1.8 | 40.7 ± 3.4 | 18.7 ± 1.5 | 4.44 ± 0.7 | 4.88 ± 0.7 |
| | | | 50 | −0.32 | 34.07 | | | 14 | | | | | | |

*(continued on next page)*

**Table 1** (*continued*)

| Station | Period of seabed exposure (yr)* | Distance from glacier front (km) | WaterDepth (m) | Water column properties** | | Sediment properties | | | | Sediment composition (%)*** | | | | Mean grain size (ϕ) | Sorting (ϕ) |
|---|---|---|---|---|---|---|---|---|---|---|---|---|---|---|---|
| | | | | AnnualMean temp. (°C) | AnnualMean salinity (psu) | TOC (n = 3) (%) | TN (n = 3) (%) | n | Gravel | Sand | Silt | Clay | | | |
| | | | | | | 0.30 ± 0.04 | 0.029 ± 0.008 | | 11.6 ± 19 | 15.9 ± 3.4 | 44.2 ± 9.5 | 28.3 ± 6.1 | 5.53 ± 2.0 | 3.83 ± 2.0 |
| | | 70 | | −0.38 | 34.09 | 0.27 ± 0.10 | 0.026 ± 0.008 | 16 | 18.5 ± 7.0 | 17.2 ± 1.5 | 39.0 ± 3.4 | 25.2 ± 2.2 | 4.94 ± 0.7 | 4.67 ± 0.7 |
| | | 90 | | −0.58 | 34.15 | 0.26 ± 0.05 | 0.026 ± 0.01 | 22 | 7.6 ± 4.3 | 12.2 ± 0.6 | 44.3 ± 2.1 | 35.9 ± 1.7 | 6.32 ± 0.4 | 3.36 ± 0.5 |

by subtracting total inorganic carbon (TIC) from TC. TIC was measured using a CM5017 $CO_2$ coulometer attached to a CM5240 auto-acidification module (UIC Inc.).

### 2.4. Statistical analyses

Multivariate statistical techniques were applied to biotic and abiotic
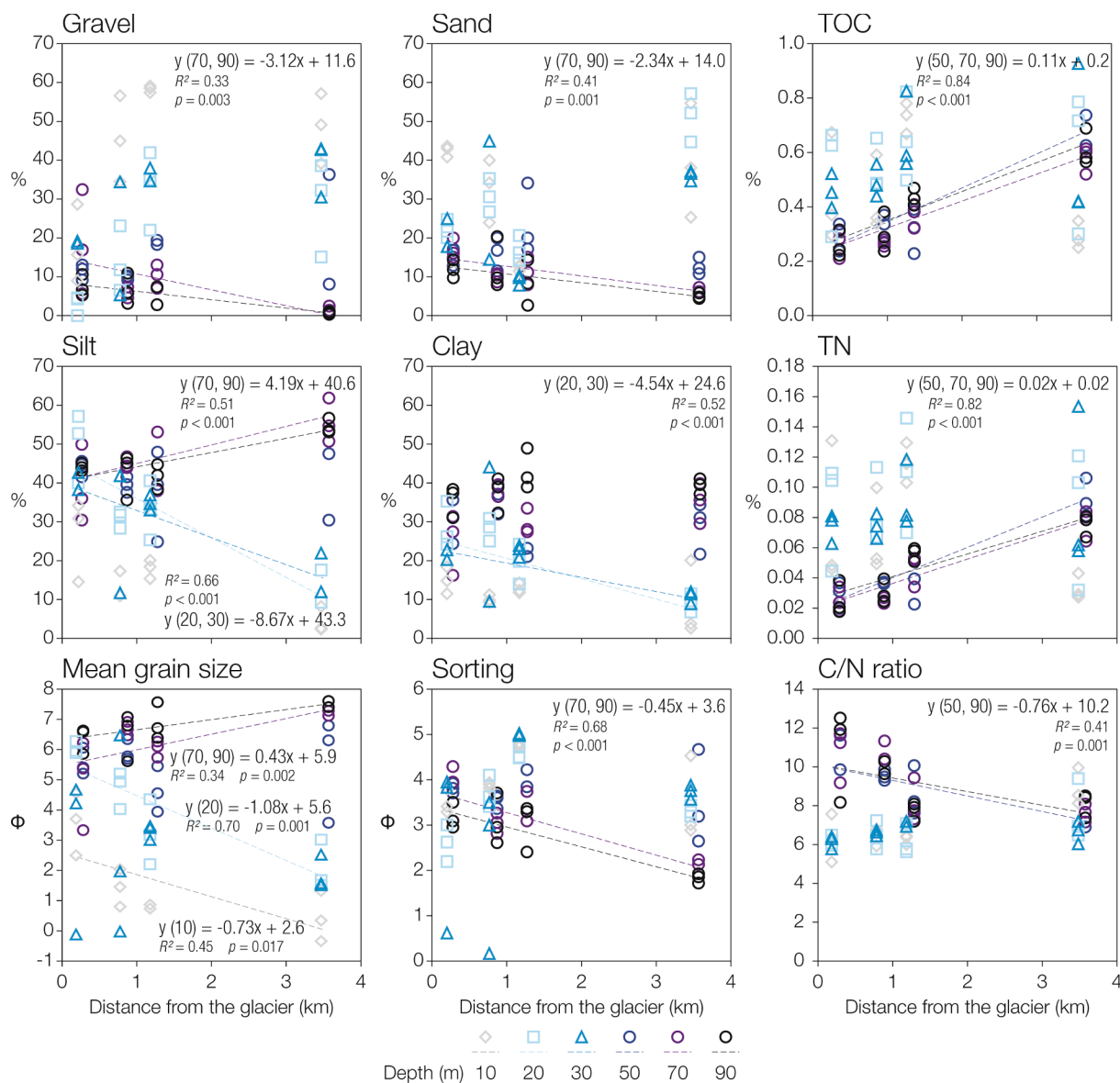


**Fig. 2.** Spatial variations in sediment properties across stations (MC5, MC4, MC3, and MC2) and water depths (10, 20, 30, 50, 70 and 90 m). All replicate data from each station were plotted in terms of distance from the glacier, showing stations MC5, MC4, MC3, and MC2 from left to right. Regression lines that are statistically significant are plotted. Data from lines representing statistically insignificant differences (analysis of covariance, ANCOVA, $p > 0.05$) were pooled for construction of a single regression equation.
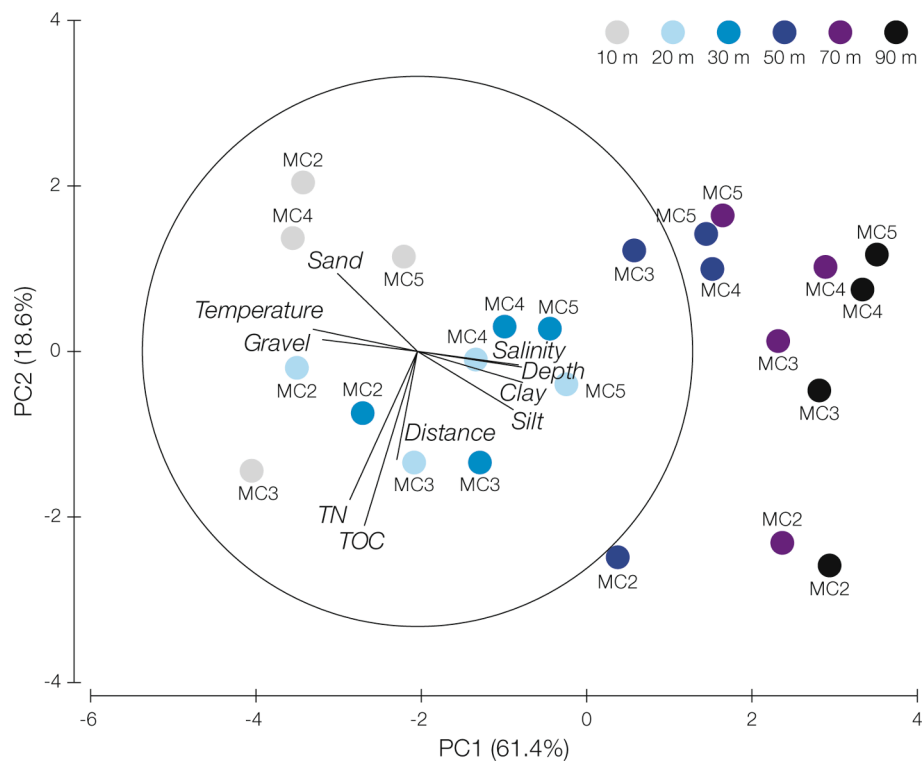
**Fig. 3.** Principal component analysis (PCA) plot showing spatial variations in environmental parameters among stations (MC2, MC3, MC4, and MC5) and depths (10–90 m). Constructed based on the data presented in Table 1.

data, and the results of each analysis were used collectively to identify the key environmental variables structuring ascidian communities in this glacial cove. Similarity of assemblages (total epibenthic fauna and ascidian communities, respectively) among stations and depths was assessed using non-parametric multidimensional scaling (MDS) analysis. A two-dimensional ordination plot was produced based on the Bray-Curtis similarity matrix constructed from square-root transformation of the abundance data (Table S1). Statistical differences among assemblages at different stations or depths were tested using one-way analysis of similarities (ANOSIM) and the similarity percentage procedure (SIMPER). SIMPER was also used to determine the species contributing most to those differences. Principle component analysis (PCA) was performed to identify the groups of samples (stations and depths) with similar environmental characteristics. Finally, biota-environment (BIOENV) analysis was used to determine which environmental parameters best explain the distribution of ascidians. All abiotic variables were normalized prior to analysis. Univariate non-parametric analyses (Kruskal-Wallis test and Mann-Whitney $U$ test) were performed using PASW Statistics (version 18.0). All other statistical analyses were performed using PRIMER software (version 6.1.16) (Clarke and Gorley, 2006).

### 2.5. *Supporting datasets*

Air temperature (1988–2018), suspended particulate matter (SPM, 1996–2018), and seawater temperature and salinity (2011–2019) data, were obtained from the long-term environmental monitoring dataset for King Sejong Station.

### 3. Results

#### 3.1. *Environmental characteristics of the study area*

The environmental characteristics of each station at various depths are summarized in Table 1. Analysis showed that over the last six

decades the period (in years) of seabed exposure after deglaciation were highly correlated with the longitudinal distance to the present glacier front (Y = 26.415X + 0.782, $r^2$ = 0.89, p < 0.001, where X is the distance to the glacier and Y is the estimated years after retreat). The period of seabed exposure after glacial retreat at the stations in the inner cove was estimated into a narrow range of years based on the satellite images (Fig. 1). No information, however, was available on glacier position before 1956, and MC2 was assumed as exposed for at least 62 years.

The monitoring data obtained from the station (2011–2019) (see the Section 2.5) showed that distinct spatial and temporal gradients of seawater temperature and salinity developed in the surface layer (<20 m) during the summer months (December through February) due to inflow of glacial meltwater. However, the annual mean values showed only slight differences among stations (−0.3 to −0.4 °C, 33.9–34.0 psu) and among depths (−0.3 to −0.6 °C, 33.9–34.1 psu). On the other hand, sediment properties exhibited distinct spatial variations (Fig. 2, Table 1). For example, gravelly sediments mixed with sand dominated (>60–88%) to a 10 m depth at all stations, while silt and clay comprised the largest portion of sediment at greater depths. Silt and clay contents increased most dramatically toward the bottom (p < 0.01, regression analysis) at the remote site (MC2) (means = 12% at 10 m, 25 at 30 m, 71 at 50 m, and 94 at 90 m), while these contents varied less (40–80%) with depth at the site closest to the glacier (MC5).

Notably, silt and clay contents increased toward the glacier front at <30 m depths, but these contents showed an opposite trend in deeper waters. In particular, silt contents increased distinctly toward the outer cove, reaching the highest values at 70–90 m at MC2. At 70–90 m depth at station MC2, silt and clay dominated (>90%) the bottom sediment, comprising clayey silty sediment, while at the same depth range of station MC5, silt and clay comprised <80% of sediment and substantial portions (>20–36%) of gravel and sand were present. As a result, the sediments at 70–90 m at MC2 were the finest (means = 7.2 phi at 70 m, 7.4 at 90 m) and best sorted (means = 2.1 phi at 70 m, 1.8 at 90 m) across the entire cove. Overall, the sediment composition, mean grain size, and level of sorting among the stations differed more distinctly in

**Table 2**
List of ascidian taxa occurring at depths of 10–90 m in Marian Cove constructed from the images taken by ROV survey in December 2017 to February 2018.

| Ascidian species | Description in Moon et al., 2015 | Life mode | Morphological description |
|---|---|---|---|
| *Molgula pedunculata* | | Solitary | Fairly translucent, with long stalk or peduncle |
| *Cnemidocarpa verrucosa* | | Solitary | Brown or yellow to white and translucent, cylindrical and covered with protuberances |
| *Ascidia challengeri* | Ascidiacea sp.14 Ascidiacea sp.15 | Solitary | Translucent and smooth tunic, body lying flat on the bottom without stalk, oral siphon at the end of body, atrial siphon at 1/4–1/3 of body length |
| *Tylobranchion speciosum* | Ascidiacea sp.12 | Colonial | Translucent, short peduncle, club-shaped head, occurs as epibiont on other ascidians and algae |
| *Pyura setosa* | Ascidiacea sp.2 | Solitary | Grayish to brownish, ovoid shape with surface completely covered in flexible bristles |
| *Corella antarctica* | Ascidiacea sp.4 | Solitary | Translucent, flat and smooth tunic |
| *Distaplia* sp. | Ascidiacea sp.10 | Colonial | Translucent and yellow, cotton ball-shaped with slender stem, occurs in Magellan region, sub-Antarctic islands, South Shetland Islands, and Antarctic Peninsula |
| *Sycozoa sigillinoides* | | Colonial | Thick peduncle, cylindrical head |
| Ascidiacea sp.16 | | Solitary | Translucent and soft tunic, elliptical body, attached to surface of other organisms |
| Ascidiacea sp.17 | | Colonial | Yellow or orange, irregular shape, usually settled on other organisms |
| *Aplidium* cf. *radiatum* | | Colonial | Round shape, settled on muddy or sandy bottom |
| *Pyura* cf. *discoveri* | | Solitary | Brown, hard, corrugated tunic, triangular body shape with protruding siphons away from each other |
| *Pyura* cf. *bouvetensis* | | Solitary | Spherical body with long stiff peduncle, distinct oral and atrial siphons |
| *Pyura* sp.1 | | Solitary | Elliptical body with long stiff peduncle, distinct siphons |

the deeper waters, while these variations with water depth were most distinct at MC2, the most distant site from the glacier front.

As with sediment grain size, sediment TOC and TN contents and C/N ratios varied significantly among stations and water depths (Fig. 2). In shallow waters (20–30 m), no significant differences were observed in organic matter content or C/N ratio among stations. However, in deep waters (70–90 m), distinct differences were found among stations; the organic contents tended to decrease toward the inner cove and reached their lowest values at MC4 and MC5; C/N ratios varied from 6.2 to 10.9 in the opposite manner to organic content, with the highest values (9.6–10.9) at MC4 and MC5. Organic matter contents were significantly higher in shallow waters (<30 m) (TOC: 0.43–0.73%, TN: 0.068–0.12%) compared to those at 50–90 m (0.26–0.44%, 0.025–0.056%) (Mann-Whitney $U$ test, $p < 0.001$) at all stations except MC2. At MC2, organic contents in deep waters (TOC: 0.58–0.69%, TN: 0.076–0.093%) were as high as those at 20–30 m depth (TOC: 0.59–0.60%, TN: 0.085–0.091%). Likewise, the C/N ratios at MC2 were similar across all water depths investigated. Overall, the quantity and quality of organic matter decreased clearly toward the glacier front in deep waters (50–90 m), but the differences in shallow waters were less distinct.

These distinct environmental variations observed among stations and water depths are well reflected in the PCA plot (Fig. 3). The first principal component axis (PC1) was explained primarily by depth, water column properties and sediment grain size (coefficient >0.3), and could classify the habitat largely into three depth ranges (10, 20–30 m and 50–90 m). In addition, PC2 explained the differences among the stations mainly through distance from the glacier, TOC and TN (coefficient >0.4). Notably, the differences among stations were more prominent in deep waters (50–90 m) than in shallow waters. The environmental characteristics observed at depths of 50–90 m at MC2 differed markedly from those at the same depths at other stations (MC3, MC4, and MC5) in the inner cove, while the differences among stations in shallow waters were much smaller. Thus, multivariate and univariate analyses on habitat properties demonstrated a major shift in habitat properties between the depths of 30 and 50 m (Figs. 2 and 3) and showed that properties were far more differentiated among stations in deeper waters (>50 m).

*3.2. Ascidian contribution to the spatial variations of total epibenthic megafauna*

A total of 64 epibenthic megafaunal taxa (16 phyla, 11 classes, 6 families, 16 genera, and 15 species) were identified from the ROV images (Table S1). Ascidians and echinoderms were the most diverse (14 taxa, respectively) followed by sponges (11 taxa), bryozoans (8 taxa) and cnidarians (7 taxa). Among 14 ascidian taxa observed (nine solitary and five colonial), seven were identified to the level of species, five to genus, and two to class (Table 2). These 14 ascidian taxa exhibited wide variations in size (from tens of centimeters to less than one), color, body form (stalked, non-stalked, and irregular), and life mode (solitary and colonial). In addition, ascidians were the most abundant group (mean = 42 inds·m$^{-2}$) accounting for 63% of total megafauna throughout the cove, followed by annelids (16%), and echinoderms comprised only 5% of the total. Overall, ascidians were the most diverse and most abundant taxonomic group.

The species number and abundance of megabenthic fauna varied distinctly among the stations and with water depths. The highest species number (33 taxa) was observed at 70 m of MC2, while the highest abundance occurred at 30 m (mean = 195 inds·m$^{-2}$) of MC5. Ascidians also showed similar patterns with those of total benthos with the highest species number (8 taxa) at 70 m of MC2 and the highest abundances at 30 m of MC5 (mean = 127 inds·m$^{-2}$) and 50 m of MC2 (mean = 128 inds·m$^{-2}$) (Fig. 4).

Similarity between the total epibenthic and ascidian assemblages was further assessed using MDS plots. Total benthic assemblages were clearly distinguished by longitudinal distance from the glacier and water depth (Fig. 5a) (ANOSIM test: global $R = 0.509$, $p = 0.001$). The assemblages at MC4 and MC5 in the inner cove were more closely clustered than those at either MC3 or MC2, and MC2 assemblages were most distinctly discriminated from those of other stations. Among depths, the assemblages at 20 m were distinct from those in deeper waters at all stations, while those in deeper waters (30–90 m) were closely grouped at all stations except MC2. Notably, the assemblages at MC2 were clearly distinguished, with depth to 70 m (global $R = 0.631$, $p = 0.001$).

Ascidians showed assemblage patterns (ANOSIM test: global $R = 0.394$, $p = 0.001$) very similar to those of total epibenthic megafauna (Fig. 5b). SIMPER analysis revealed that ascidians contributed most (36–69%) to the dissimilarity of the total megafaunal communities among stations and water depths, except at 20 m depth in MC3, where the tube-building polychaete Terebellidae sp. (25% to the total) and the sea urchin *Sterechinus* sp. (24%) were as abundant as ascidians (25%) (Table S1). Although echinoderms were as taxonomically diverse as ascidians, they showed less similarity in assemblage patterns (global $R = 0.125$, $p = 0.001$) (Fig. 5c) and contributed only 5–30% to the dissimilarities of the total benthos. Notably, the ascidian assemblage at 30 m of MC2 clustered closely with those observed at 30–90 m of MC4 and MC5 (Fig. 5b).

## Number of taxa

### Total megafauna        Ascidians

## Abundance (inds · m⁻²)

### Total megafauna        Ascidians
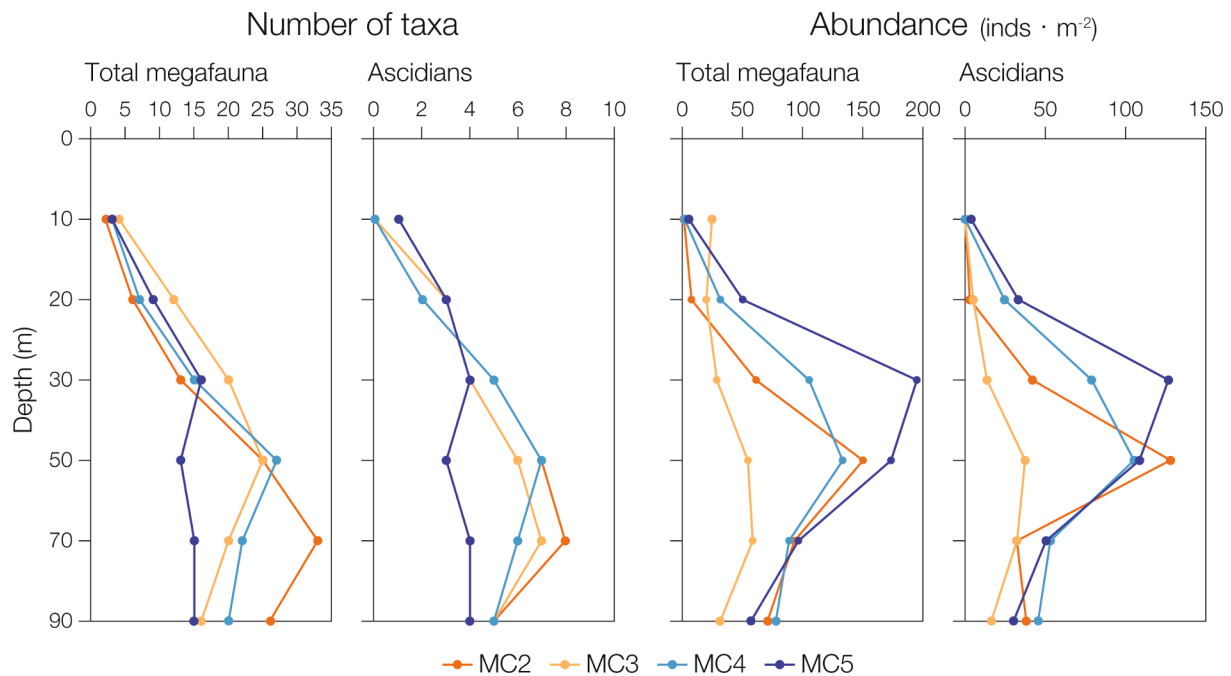


**Fig. 4.** Ascidian abundance and number of taxa present across various depths (10, 20, 30, 50, 70, and 90 m) at four stations (MC2, MC3, MC4, and MC5) in comparison with those of the total megafauna. Total number of taxa represents total sum of taxa occurred at a specific depth of each station. Only mean values represent for abundance (refer to Table S1 for the details of data).

### 3.3. Spatial patterns of ascidian distribution

#### 3.3.1. Abundance, species composition and diversity

Ascidian abundance, species composition and diversity varied greatly among stations and water depths (Fig. 6, Table S1 and Table S2). Few ascidians occurred at <10 m depth, with only one species (*Cnemidocarpa verrucosa*) recorded at MC5. A moderate increase in density, mostly related to *C. verrucosa* (>90% to the total) was observed at 20 m in the innermost cove station, near the glacier (means = 25 inds·m⁻² at MC4, 31 inds·m⁻² at MC5), while ascidians remained at low levels at more distant sites (means = 5 inds·m⁻² at MC3, 3 inds·m⁻² at MC2). With increasing water depth, the ascidian density and biomass increased sharply, reaching a peak at 30–50 m depth at all stations.

Overall, *Molgula pedunculata* (41% to the number) was the most abundant ascidian in the cove, followed by *C. verrucosa* (24%) and *Ascidia challengeri* (18%). In terms of biomass, however, *C. verrucosa* (61%) outweighed *M. pedunculata* (19%) and *A. challengeri* (14%) at almost all stations and depths. Moreover, *M. pedunculata* and *C. verrucosa* predominated at the sites near the glacier and at shallow water (<30 m), while *A. challengeri* was most abundant at the distant site (MC2) and at deeper water (>50 m).

Ascidians were most abundant at the innermost station (MC5) near the glacier in terms of both density (~264 inds·m⁻²) and biomass (~15.7 kg·m⁻²). The peak abundance (means = 127 inds·m⁻² and 6.3 kg·m⁻²) was observed at 30 m depth of this station, where *M. pedunculata* (mean = 83 inds·m⁻², max = 144) and *C. verrucosa* (37 inds·m⁻², max = 108) together comprised 95% of total ascidians. *M. pedunculata* and *C. verrucosa* flourished across all depths at MC5 for the majority of ascidians present (83–100% to the total number, 87–100% to the total biomass). *M. pedunculata* and *C. verrucosa* also predominated down to a depth of 30 m at all stations, but their abundance tended to decrease toward the outer cove. The peak densities of *M. pedunculata* (mean = 18 inds·m⁻², max = 72 at 30 m) and *C. verrucosa* (mean = 16 inds·m⁻², max = 52 at 30 m) at the most distant site (MC2) were several times lower than those in the inner cove.

Unlike the ascidian communities at the ice-proximal zone and the shallow water, those in the deeper waters (>50 m) differed markedly

with longitudinal distance from the glacier front. More diverse taxa were observed toward the outer cove, with the highest species richness (8 taxa) at 70 m of MC2. Moreover, at MC2, the species richness and composition differed distinctly with water depth (Figs. 6 and 7). *M. pedunculata* and *C. verrucosa* dominated to the depth of 30 m, but decreased sharply (<2 inds·m⁻² each) to 70 m, and none were observed at 90 m. At 50 m, *A. challengeri* (mean = 53 inds·m⁻², 41% to the total) was most abundant, followed by *Aplidium* cf. *radiatum* (40 inds·m⁻², 31%) and Ascidiacea sp.16 (30 inds·m⁻², 23.4%). On the other hand, at 70 m, Ascidiacea sp.17 was most abundant (12.5 inds·m⁻², 38.8%), followed by *A. challengeri* (11 inds·m⁻², 32%), while at 90 m, Ascidiacea sp.17 was most abundant (23 inds·m⁻², 59%), then *Pyura* cf. *discoveri* (9 inds·m⁻²) and *Pyura setosa* (4 inds·m⁻²).

At MC2, many individuals of the diverse taxa observed in the deep water were small in size, as compared to *M. pedunculata* and *C. verrucosa* occurring at shallow water (Fig. 7). As a result, overall ascidian biomass (mean = 3.2 kg·m⁻²) at MC2 was not proportional to the density. Ascidian density peaked at 50 m (mean = 128 inds·m⁻², max = 244) due to the presence of diverse taxa, while the biomass peaked at 30 m (mean = 5.2 kg·m⁻², max = 11.6) where the ascidian communities were predominated by large *M. pedunculata* and *C. verrucosa*.

#### 3.3.2. Differences in body size among stations

As shown in Fig. 8, size frequency distributions of three dominant ascidian species were strongly skewed to the left (skewness values >1), representing a large proportion of small size classes and a long tail with a small number of large individuals, and this trend was most prominent for *M. pedunculata* in the inner cove (MC3, MC4, and MC5). The average body size of *M. pedunculata* was several times larger (Mann-Whitney test $p < 0.001$) at the outer cove station (MC2) (mean = 79 g tww, equivalent to 20.1 cm L) compared to those in the inner cove (13–23 g tww, 6.8–9.9 cm L). In addition, ascidians in the outer cove showed a wider range of size classes (<20–280 g tww, <9.0–38.9 cm L) compared to the size range (<20–160 g tww, <9.0–29.3 cm L) observed in the inner cove. Moreover, the majority of inner cove populations (>95%) belonged to classes of <60 g tww (<17.4 cm L), while only 44% belonged to the same classes at MC2, leading to extreme kurtosis values at MC3 (5.1),

## (a) Total megafauna

2D Stress: 0.11



## (b) Ascidiacea

2D Stress: 0.08



## (c) Echinodermata

2D Stress: 0.1



--- Similarity: 60 ● MC2 ● MC3 ● MC4 ● MC5
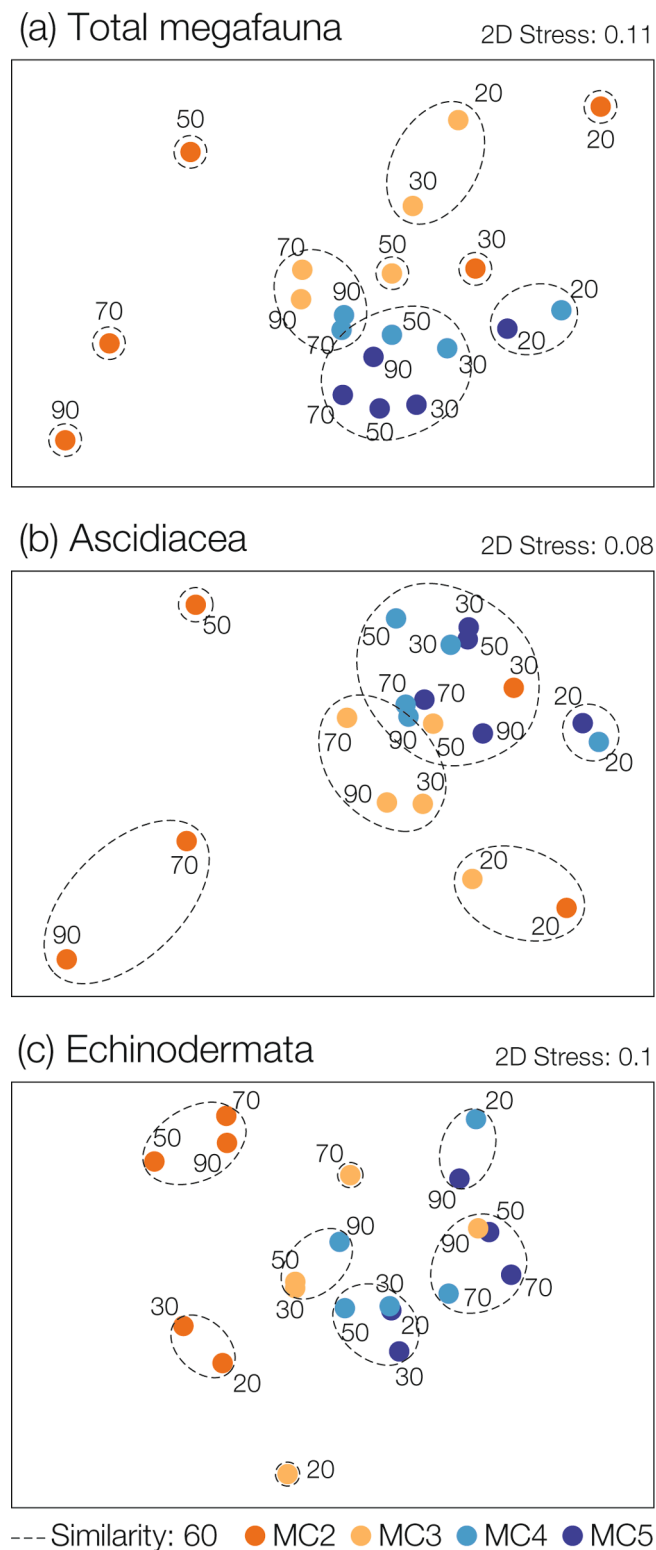
**Fig. 5.** Non-metric multidimensional scaling (MDS) plots for total epibenthic megafauna and the two dominant taxa based on Bray-Curtis similarity matrix data (Table S1). Numbers near the symbols represent water depth (m) of each habitat. Data from 10 m depth were excluded for MDS analysis, as only a few taxa were present at this depth (in the case of ascidians present only at MC5).

MC4 (4.0) and MC5 (7.6).

*C. verrucosa* showed a similar trend to *M. pedunculata*; average body sizes were several times larger (Mann-Whitney test $p < 0.01$) at MC2 (mean = 215 g tww, 14.8 cm L) than in the inner cove (MC3, MC4, and MC5) (81–115 g tww, 8.7–10.6 cm L). *C. verrucosa* also showed a broader size range (>20–640 g tww, >3.8–26 cm L) in the outer cove compared to the range (<20–460 g tww, <3.8–21.9 cm L) in the inner cove. Likewise, *A. challengeri* showed smaller body size at MC4 and MC5 than those at MC2 ($p < 0.001$) and MC3 ($p < 0.05$), but this trend was not as prominent as those of *M. pedunculata* and *C. verrucosa*.

Despite having much lower mean density values (18 and 16 inds·m$^{-2}$, respectively), the peak biomass values (at 30 m) of *C. verrucosa* and *M. pedunculata* at MC2 (3.5 kg·m$^{-2}$ and 1.4 kg·m$^{-2}$) were disproportionately high compared to values at MC5 (4.3 kg·m$^{-2}$ and 1.9 kg·m$^{-2}$), where the densities of the two species were several times higher (82 and 37 inds·m$^{-2}$, respectively) (Fig. 6). This discrepancy can be attributed to differing frequency distributions of ascidian size classes among stations (Fig. 8).

### 3.4. Relationship between ascidian assemblages and environmental parameters

BIOENV analysis was performed to determine environmental variables which best explain the ascidian distribution. Environmental variables for the analysis were chosen based on the analysis results on the habitat properties (Figs. 2, 3 and 5; Table 1). Distance from the glacier front was also added as a variable for the analysis. The high correlation between the distance to glacier and the period of deglaciation over the last six decades supported the notion that the distance may be used as a proxy of how long the seabed has been exposed after glacial retreat. Given a major shift in the habitat properties between the depths of 30 and 50 m (Figs. 2 and 3), the analysis was conducted for two subdivided depth ranges (20–30 m and 50–90 m) in addition to the entire depth range (20–90 m). The depth of 10 m was excluded from analysis, as ascidians occurred at that depth only at MC5.

The single and combined parameters that best explain the ascidian distributions in the three depth categories are listed in Table 3. Over all depths except 10 m, the most influential single variable was distance ($R = 0.446$), followed by %silt, %sand, %TOC, and the combination of these variables best explained the spatial variations of ascidian assemblages ($R = 0.584$). For shallow depths (20–30 m), in contrast, distance had little effect on the assemblages, which were mostly affected by organic contents and sediment composition. Meantime, at 50–90 m depth, %TOC ($R = 0.802$) was the most influential single factor, along with %TN ($R = 0.756$), distance ($R = 0.700$), and %silt ($R = 0.493$) in order. Of note, the combination of these variables was most influential in structuring ascidian assemblages ($R = 820$). Seawater temperature and salinity had weak correlations in all depth categories.

## 4. Discussion

### 4.1. Ascidians as a key megabenthic community in an Antarctic fjord

A total of 64 taxa were described from the ROV images in this study, which was much less than the number of taxa described by direct sampling at <35 m depths in the previous study (117 taxa in Moon et al., 2015). That is because the ROV captured only two-dimensional images, and fauna covered by or underneath other organisms could not be detected in the images. In addition, small bivalves, bryozoans and amphipods were not discernable in the images. Nonetheless, most common epibenthic megafauna (e.g. *M. pedunculata*, *C. verrucosa*, *Odontaster validus*, *Sterechinus* sp., *Flabegraviera* sp., *Nacella concinna*, *Neobuccinum eatoni*, *Parborlasia corrugatus*, and *Serolis* sp.) that occur in shallow Antarctic waters (Sahade et al., 1998; Barnes et al., 2006; Siciński et al., 2011) were identified from the images (Table S1). As for the ascidians, the total number of species (14) described from the images are
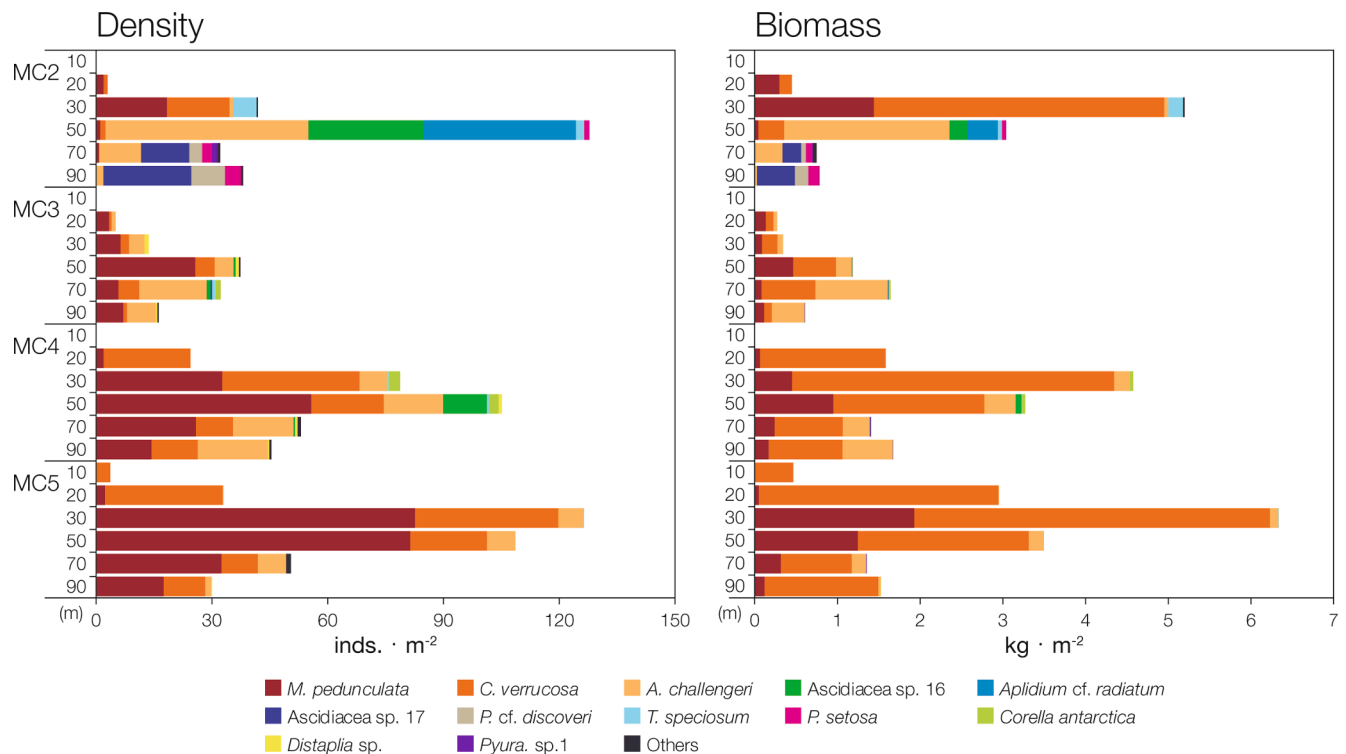
**Fig. 6.** Ascidian abundance and composition among various depths (10, 20, 30, 50, 70, and 90 m) at four stations (MC2, MC3, MC4, and MC5) in Marian Cove (MC). Most density peaks occurred at 30 or 50 m, while biomass peaks at 30 m were observed at all stations except MC3. Others include ascidian taxa that account for <3% of the total number of ascidian individuals at all stations. The horizontal bars indicate mean values. Refer to Tables S1 and S2 for the data and standard errors.

comparable to those identified by direct samplings in adjacent nearshore bays in KGI, such as PC (17 in Tatiàn et al., 1998), and Admiralty Bay (16 in Siciński et al., 2011). Thus, despite some disadvantages (e.g., size limitation for taxonomic identification, underestimation of abundance and species richness), the ROV survey proved to be an efficient and reliable tool in this glacial cove for investigating large epibenthic megafauna such as ascidians, providing sufficient quantitative data to determine their distributional patterns.

Overall, the ROV survey revealed that ascidians were the most diverse (14 out of 64 taxa captured in the ROV images) and most abundant (mean = 42 inds·m$^{-2}$, 63% to the total) taxa among the epibenthic megafaunal communities in this glacial cove. Furthermore, the ascidian community was most responsible for the spatial variations of the total megafaunal communities across the cove (Fig. 5), suggesting that ascidians could be utilized as a key community representing the megafaunal benthic community in this fjord and other similar Antarctic nearshore environments.

### 4.2. Ascidian assemblages in the ice-proximal zone

The ice-proximal zone (the area in the innermost cove near the glacier front) represents apparently most unstable habitat for benthic organisms. Retreating glaciers are accompanied by generation of hundreds of floating ice pieces and massive inflow of turbid melt-water, consequently impacting benthic inhabitants, especially in shallow seabed. Ice-related disturbance and sedimentation have been considered as two principal disturbances associated with the retreat of marine-terminating glaciers in the coastal areas of WAP, acting detrimentally on benthic communities, particularly in shallow waters (Smale and Barnes, 2008; Moon et al., 2015; Sahade et al., 2015). These two types of disturbance are also likely acting on the benthic communities in MC. Based on the observations on sea surface coverage by floating and/or grounded ices, Moon et al. (2015) reported that floating ice occurred at a much higher density in the inner cove, and suggested that scouring by

ices generated from glacier carving is most intense close to retreating glaciers and is attenuated toward the outer cove.

Sedimentation also appears to be most intense at the area close to the glacier front. The high silt and clay contents throughout almost the entire water column at MC5, strongly indicated that heavy sedimentation of terrigenous particles nearly reached the bottom in the area near the glacier. Silt and clay contents decreased significantly toward the outer cove in shallow waters (<30 m) apparently as a result of decrease of turbid meltwater influence. The photographic images (Fig. 7), where the seabeds and organisms were covered by fine sediment, support the idea that sedimentation is most intense close to the retreating glaciers. Previous studies in the cove also reported that sedimentation of terrigenous particles (mostly clastic silt-sized) carried by melt water occurred heavily in the ice-proximal zone (Yoon et al., 1997, 1998; Yoo et al., 2015).

Notably, ascidians were most abundant at this area, where physical disturbance associated with glacial retreat was extremely severe. In particular, the two species, *M. pedunculata* and *C. verrucosa*, predominated across all depths at sites near the glacier with the peak abundances at 30 m (Fig. 6). Furthermore, at the depth of peak abundance, most individuals of the two species were very small compared to those observed at the same depth from the distant site in the outer cove (MC2) (Fig. 8), corroborating the idea that communities near the glacier front were at an early colonization stage. The predominance of small *M. pedunculata* and *C. verrucosa* individuals also suggested that they are short-lived in the ice-proximal zone. However, the high densities and biomass of small *M. pedunculata* and *C. verrucosa* individuals indicated that their populations could be maintained through rapid colonization and growth outweighing mortality. *M. pedunculata* and *C. verrucosa* are known to grow at least several times faster than other ascidian species, while they have relatively short life spans (~3.4 yrs) compared to other species (e.g., *A. challengeri* at ~11 yrs) (Kowalke et al., 2001).

Rapid colonization by *M. pedunculata* and *C. verrucosa* at high densities has frequently been reported in Antarctic nearshore embayments
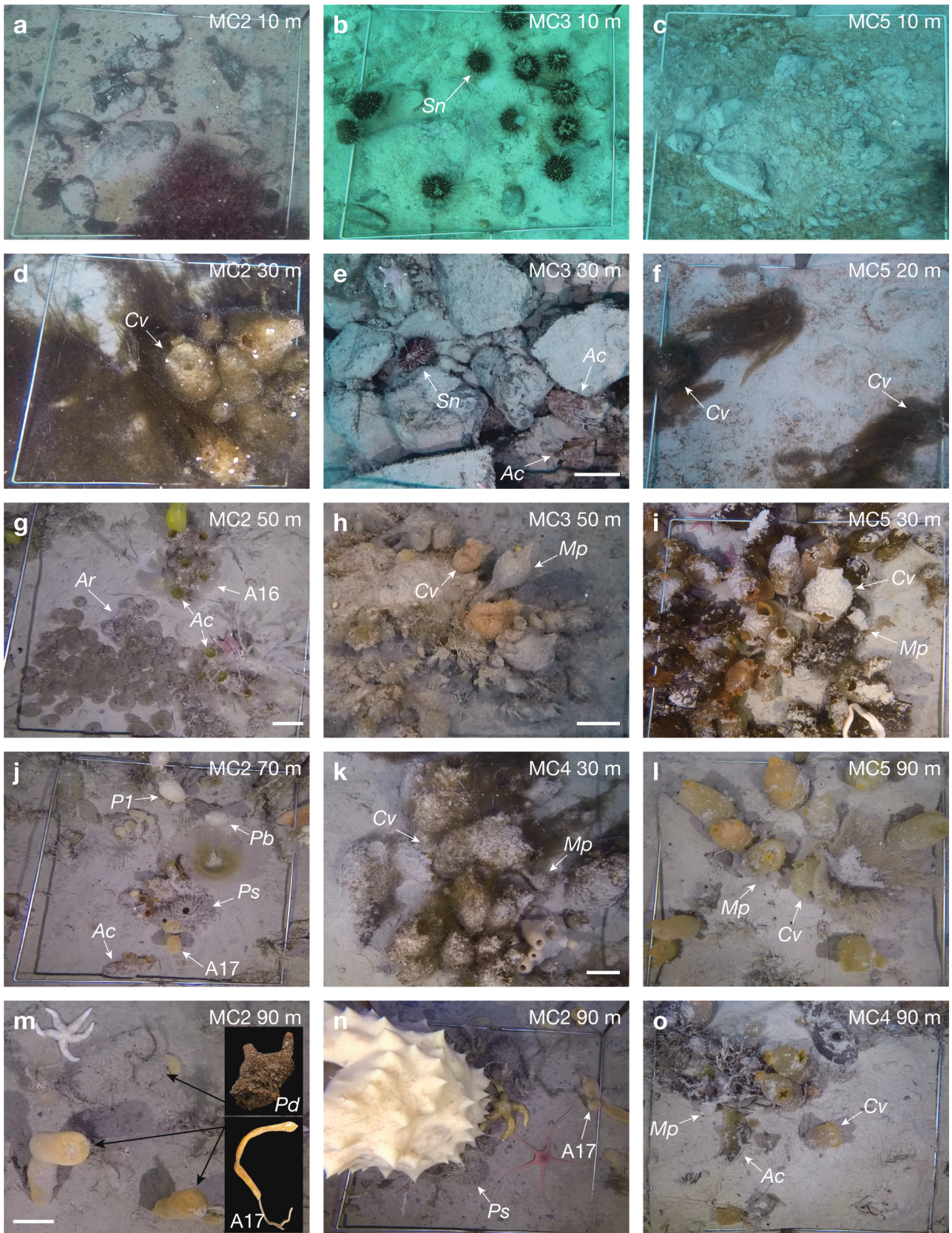
*(caption on next page)*

**Fig. 7.** Images of ascidians within a quadrat (50 × 50 cm) taken by a ROV, showing distinct shifts in key taxa and the diversity of ascidian communities among stations and water depths in Marian Cove. (a, b) bottom substrates dominated by gravel at 10 m; sea urchins occurring at the highest numbers at this depth at MC3; (c) seabed covered by sand and silty sediment indicating heavy sedimentation near glacier (d) Ascidian communities, mostly comprised of *Molgula pedunculata* and *Cnemidocarpa verrucosa,* covered by dense blooms of the benthic diatom *Paralia* sp. (refer to Ha et al., 2019); (e) Relatively low ascidian abundance on boulder-sized substrate in shallow waters at MC3; (f) *C. verrucosa* population entangled with massive growth of benthic diatom and the surrounding bare seabed covered with a thick layer of muddy sediment at 20 m depth, indicating heavy sedimentation at this site; (g) *A. challengeri, Aplidium* cf. *radiatum* and Ascidiacea sp.16 population dominating at 50 m at the distant site; (k, i) *M. pedunculata* and *C. verrucosa* predominating at 30 m depth in the inner cove (MC4, MC5); (h, l, o) *M. pedunculata* and *C. verrucosa,* less abundant but still dominating at 50–90 m in the inner cove; (j, m, n) Diverse taxa occurring at 70–90 m at MC2. Large hexactinellid sponges commonly occurred together. *Mp*: *M. pedunculata*; *Cv*: *C. verrucosa*; *Ac*: *A. challengeri*; *Pd*: *P.* cf. *discoveri*; *Ps*: *P. setosa*; *Pb*: *P.* cf. *bouvetensis*; *Ar*: *Aplidium* cf. *radiatum;* A16*:* Ascidiacea sp.16; A17: Ascidiacea sp.17; Sn: *Sterechinus* cf. *neumayeri*. Scale bars: 5 cm.
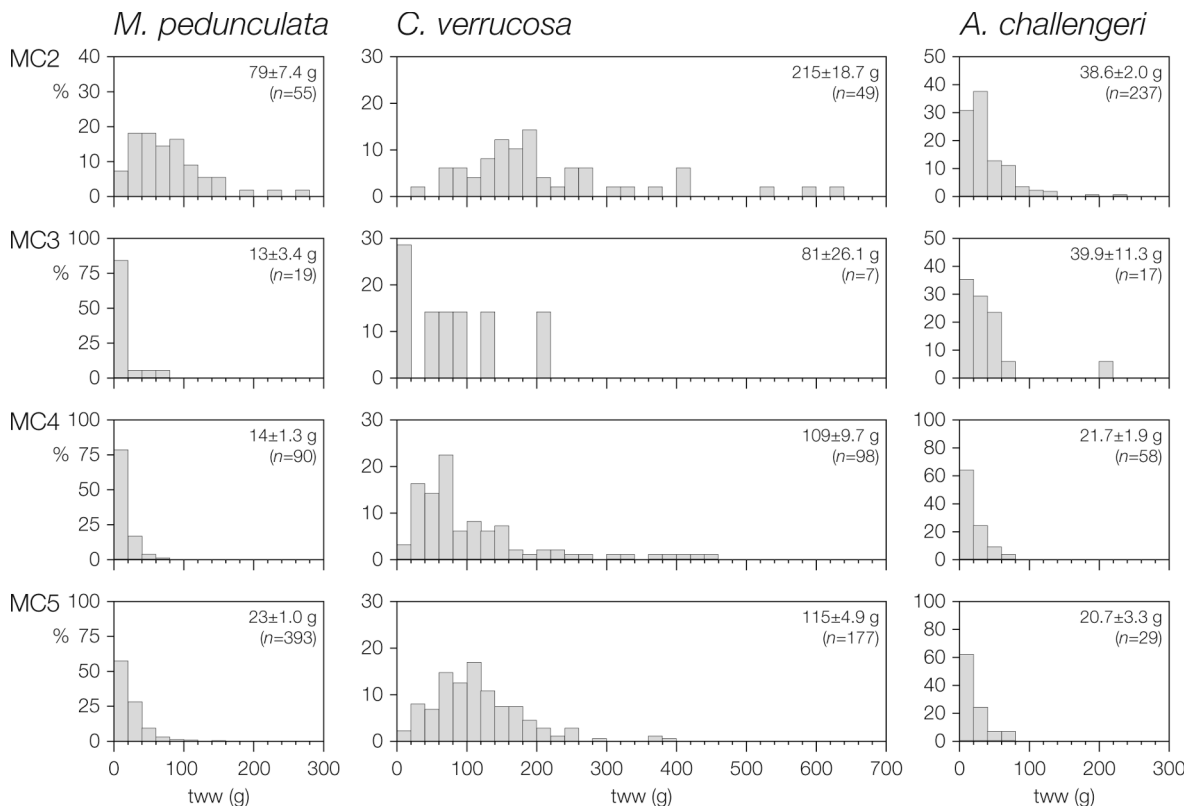


**Fig. 8.** Comparison of size frequency distributions of three ascidian species among stations (MC2, MC3, MC4, and MC5) at their depth of peak abundance (*M. pedunculata* and *C. verrucosa* at 30 m, *A. challengeri* at 50 m). Size classes were determined based on total wet weight (tww), which was determined from body width or body length measurements obtained from ROV-acquired images using allometric relationships (refer to the Fig. S2 for the details). Figures inside the plots are mean ± standard error. *n*: number of replicates.

undergoing marine-terminating glacial retreat (Sahade et al., 1998; Lagger et al., 2018). In the adjacent PC, very high numbers of ascidians (~310 inds·m$^{-2}$) colonized a newly exposed area (<30 m) after glacial retreat, with *M. pedunculata* and *C. verrucosa* together constituting the majority of colonizing ascidians (~220 inds·m$^{-2}$, >70% to the total) (Lagger et al., 2018). In this study, we observed similar ascidian densities (~264 inds·m$^{-2}$) and the predominance of the same two species (~252 inds·m$^{-2}$) at similar environments in MC. Thus, the findings from this study strongly suggested that the highest ascidian abundance at sites near the glacier front is due to rapid colonization of the two opportunistic species that have competitive advantages over other species for newly exposed and highly disturbed habitats following glacial retreat.

### 4.3. Physical disturbance structuring ascidian communities in shallow habitats

In addition to their dominance at the innermost sites, the two opportunistic ascidian species (*M. pedunculata* and *C. verrucosa*) predominated (79–100% to the total) down to a depth of 30 m at all stations across the cove, indicating that shallow habitats in the cove were highly disturbed. Notably, the ascidian assemblages at 30 m at station MC2 in the outer cove clustered closely with those at 30–90 m at MC4 and MC5 in the innermost cove (Fig. 5b), apparently due to the predominance of *M. pedunculata* and *C. verrucosa*, which had comparable abundance values.

The shallow habitats showed much less distinct variations in the environmental properties across the stations, as compared to the deep habitats (Figs. 2 and 3, Table 1), indicating that major determinants or forces structuring ascidian communities are different from those in the deep habitats. The most-likely cause is ice scouring, which is prevalent throughout the year in the Antarctic nearshore areas irrespective of glacial retreat. Ice scouring is known to be most intense at <15–20 m in Antarctic nearshore areas, resulting in low abundance and diversity of benthic communities at those depths (Smale et al., 2008; Barnes and Souster, 2011; Barnes, 2017). Likewise, in this study, abundances of ascidian as well as other taxa were very low at <20 m at all stations (Table S1), supporting the idea that physical disturbance due to ice scouring is one major force structuring benthic communities in this cove.

Overall physical disturbance in shallow waters, however, was apparently much more severe at the site nearest the glacier front due to

**Table 3**

Summary of biota-environment (BIOENV) analysis of the relationships between environmental factors and ascidian assemblages in Marian Cove. *R*: Spearman correlation coefficient. * indicates the best results. *p* < 0.01.

| Depth | Number of factors | R | Environmental factors | | | |
|---|---|---|---|---|---|---|
| 20–90 m | 1 | 0.446 | Distance | | | |
| | 1 | 0.345 | Silt | | | |
| | 1 | 0.268 | Sand | | | |
| | 1 | 0.247 | TOC | | | |
| | 1 | 0.222 | Salinity | | | |
| | 1 | 0.204 | Gravel | | | |
| | 1 | 0.189 | Depth | | | |
| | 1 | 0.188 | Temperature | | | |
| | 1 | 0.137 | Clay | | | |
| | 1 | 0.104 | TN | | | |
| | 3* | 0.584 | Distance | Sand | TOC | |
| | 4* | 0.584 | Distance | Sand | Silt | TOC |
| | 3* | 0.582 | Distance | Sand | Silt | |
| | 2* | 0.580 | Distance | Silt | | |
| | 3* | 0.578 | Distance | Silt | TOC | |
| 20–30 m | 1 | 0.573 | TOC | | | |
| | 1 | 0.286 | Sand | | | |
| | 1 | 0.252 | TN | | | |
| | 1 | 0.155 | Temperature | | | |
| | 1 | 0.117 | Salinity | | | |
| | 1 | 0.103 | Gravel | | | |
| | 1 | 0.045 | Clay | | | |
| | 1 | −0.027 | Distance | | | |
| | 1 | −0.251 | Silt | | | |
| 50–90 m | 1 | 0.802 | TOC | | | |
| | 1 | 0.756 | TN | | | |
| | 1 | 0.700 | Distance | | | |
| | 1 | 0.493 | Silt | | | |
| | 1 | 0.322 | Gravel | | | |
| | 1 | 0.248 | Sand | | | |
| | 1 | 0.056 | Salinity | | | |
| | 1 | −0.031 | Temperature | | | |
| | 1 | −0.100 | Clay | | | |
| | 4* | 0.820 | Distance | Silt | TN | TOC |
| | 3* | 0.819 | Distance | Silt | TN | |
| | 3* | 0.818 | Distance | Silt | TOC | |
| | 3* | 0.812 | Silt | TN | TOC | |
| | 2* | 0.802 | Silt | TN | | |

additional perturbation associated with glacial retreat (Fig. 9). Interestingly, *C. verrucosa* occurred in relatively high numbers at 20 m at the sites near the glacier front (mean = 23 inds·m$^{-2}$, max = 212 at MC4; mean = 31 inds·m$^{-2}$, max = 108 at MC5), where they outnumbered *M. pedunculata* (~2 inds·m$^{-2}$). Similar patterns were observed in the adjacent PC, where *C. verrucosa* showed much higher densities (~160 inds·m$^{-2}$) at 10–15 m depth than *M. pedunculata* (<60 inds·m$^{-2}$) along a newly exposed island, whereas *M. pedunculata* occurred with higher densities at 20–30 m, with its peak (>160 inds·m$^{-2}$) at 25 m (Lagger et al., 2018). *C. verrucosa* is known to tolerate heavy sedimentation better than *M. pedunculata* and other species (Torre et al., 2012). Thus, *C. verrucosa* appears to be most tolerant among the ascidian taxa in the cove to the physical disturbance associated with glacial retreat, which allow them colonize the extremely disturbed seabed.

With increasing water depth, ascidian abundance increased sharply, reaching its peak at 30 m (Fig. 6, Tables S1 and S2), which can be attributed primarily to reduced ice scouring and, at least in part, to enhanced food availability at this depth. BIOENV analysis revealed that the ascidian assemblages were significantly related to sediment organic carbon content, supporting the idea that food availability is an important factor structuring the shallow-water ascidian communities. Although no significant differences in sediment organic matter content (indicative of food amount) or C/N ratio (indicative of food quality) were found at <30 m, availability of other food sources appeared to be greater at 30 m than <20 m. Recent studies have reported that benthic diatom blooms overgrowing a variety of benthic filter feeders, including

ascidians, occur sporadically at depths of >20–50 m, with a peak occurrence around 30 m depth at most distances from retreating glaciers within the cove (Ahn et al., 2016; Ha et al., 2019). Ha et al. (2019) reported that these diatom blooms were intense and persistent, at least during the austral summer. Using isotopic tracers, Ha et al. (2019) further demonstrated that massive benthic diatom blooms were consumed as the primary food source by ascidians and other filter feeding benthic fauna, including sponges, bivalves, and terebellid polychaetes. In this study, we also observed widespread benthic diatom blooms at shallow seabeds particularly at ~30 m depth (Fig. 7). Benthic diatom blooms were observed even at the sites adjacent to glacier front, despite the apparent heavy sedimentation (Fig. 7f, i, k). This strongly suggested that food is not limiting for ascidian growth even at the sites close to glacier, which could explain rapid colonization of the two ascidian species at these sites.

At MC3, ascidian abundance was low relative to those in the other stations. Interestingly, *Sterechinus* sp. were observed at this site in relatively high numbers at <20 m (mean = 9.5 inds·m$^{-2}$, max = 44 at 10 m; mean = 4.7 inds·m$^{-2}$, max = 20 at 20 m). This can be attributed to substrate type. The bottom substrates of shallow waters (<30 m) at MC3 were comprised of relatively high proportions (19–46%) of cobble- (>64–256 mm) and boulder-sized (>256 mm) clastic rock fragments compared to the same depths at other stations (~20% at MC2, ~11% at MC4 and ~3% at MC5), which was likely to favor the sea urchin *Sterechinus* sp.

Overall, physical disturbance by ice scouring is apparently a most influential driver shaping ascidian assemblages in shallow habitats of this cove. In addition, food availability, bottom substrate type and species-specific tolerance to disturbance likely act differentially along the distance from the glacier and also with water depth, affecting, in part, ascidian assemblages. Nonetheless, the predominance of the two species, *M. pedunculata* and *C. verrucosa*, showed that the shallow-water communities remain at an early colonization stage regardless of the distance of the glacier front.

### 4.4. Successional shifts of ascidian communities in deep habitats

Unlike the ascidian communities at the ice-proximal zone and the shallow water, the deep ascidian community structure differed markedly with longitudinal distance from the glacier front, ranging from communities at the early colonization stage near the glacier front to more mature communities with diverse taxa at the remote site. The high correlation between the distance from the glacier front and the time after deglaciation suggests that we can infer the successional shift in the past from the spatial pattern in the present.

As demonstrated in the BIOENV analysis (Table 3), the ascidian assemblages in the deep-waters (50–90 m) were distinctly related to the distance from the glacier (Table 3), indicating a successional shift over a long-term period (for at least six decades) (Fig. 9). The analysis also revealed that ascidian assemblages were strongly related to sediment properties (composition, mean grain size, level of sorting, organic contents etc.) that varied significantly with the distance from the glacier in association with glacial retreat processes. The overall results of sediment analyses clearly showed that habitat stability increased toward the outer cove in the deep water.

Notably, the silt and clay contents in deeper water (>50 m) increased toward the outer cove, reaching their highest levels at 70 m (mean = 91%) and 90 m (94%) at MC2, despite the long distance between this station and the source of turbid meltwater. Moreover, these sediments were much better sorted (mean sorting values = 2.1 phi at 70 m, 1.8 at 90 m) and finer (mean grain sizes = 7.2 phi at 70 m, 7.4 at 90 m) at this distant site than those at the same depth of the nearest site (mean sorting values = 4.7 phi at 70 m, 3.4 at 90 m; mean grain sizes = 4.9 phi at 70 m, 6.3 at 90 m), suggesting that transport processes affect differentially various sizes of sediment particles in suspension. A meltwater plume carrying sediment particles (mostly angular silt-sized) was reported to
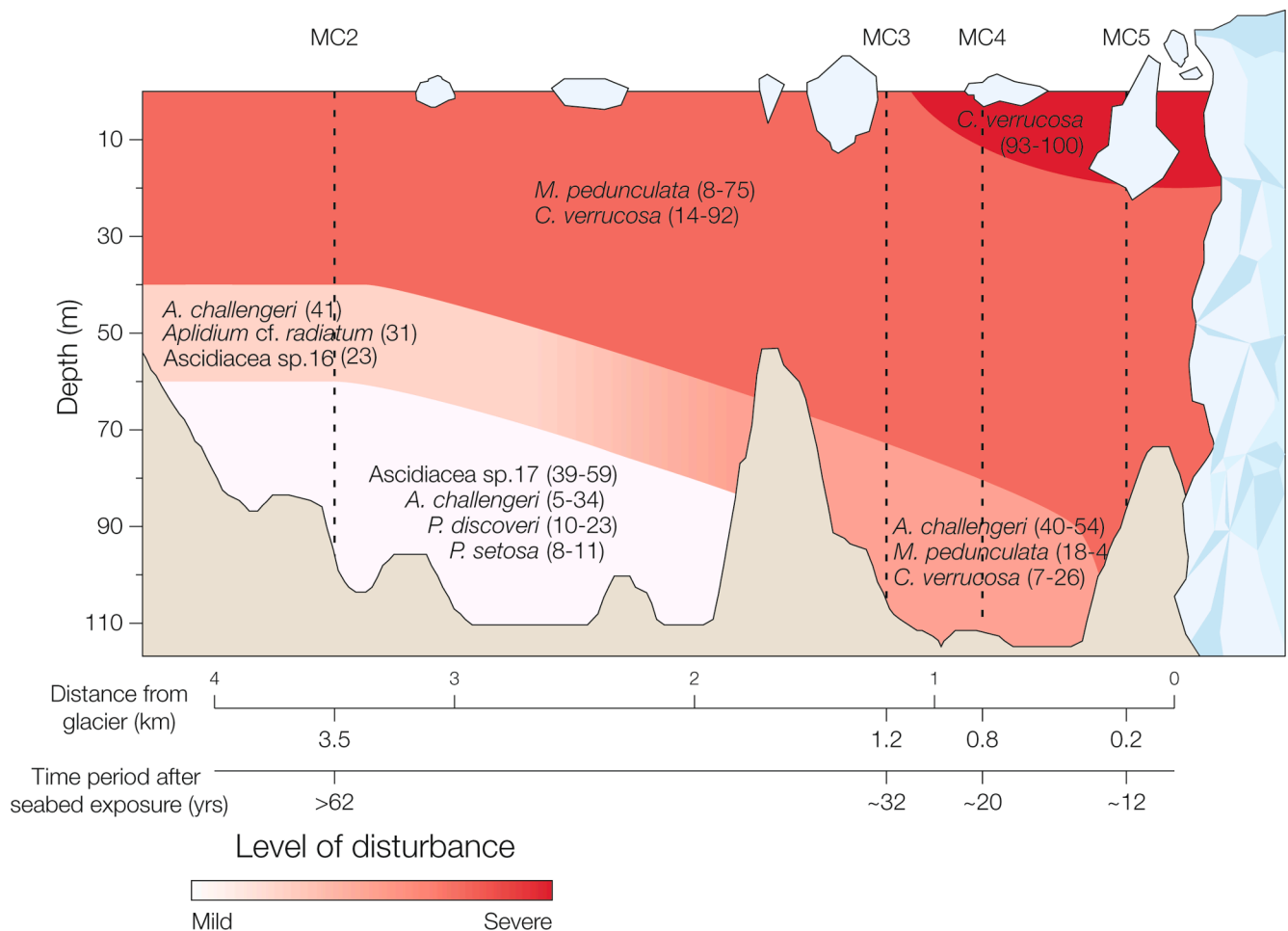
**Fig. 9.** Conceptual drawing of successional shifts in dominant ascidian taxa in Marian Cove, a fjord in the northern WAP that has been rapidly warming and deglaciating over the last six decades. This drawing illustrates how the intensity of physical disturbance, due to ice scouring and sedimentation associated with glacial retreat, acts as a key driver structuring ascidian communities. The numbers in parentheses indicate % composition.

extend far beyond the cove into Maxwell Bay (Yoon et al., 1998). While relatively large particles (e.g. sand) settle to the bottom near the melt-water source, fine particles travel longer distances, eventually dominated by fine silt and clay at greater distances (Yoon et al., 1997), which could explain the extremely high percentages of silt and clay (most sorted) observed at 70–90 m depth of MC2.

Sedimentation rates at MC2, the most distant site from the glacier front, are likely to be much lower than those at sites near the glacier, as influence of meltwater carrying sediment particles decreases with increased distance from the source. The annual average concentrations of SPM recorded at MC ranged from <3 to 30 mg·l$^{-1}$ over the last two decades (1997–2017) with higher values in the inner cove near the meltwater sources during the summer months (>28 mg·l$^{-1}$, compared to 4 mg·l$^{-1}$ at the distant site in Yoon et al., 1998; >10 mg·l$^{-1}$ compared to 1 mg·l$^{-1}$ in Ahn et al., 2004). Thus, fine and most sorted sediment in the deep waters of the outer cove may have accumulated without frequent disturbance over a long period of time, resulting in a most stabilized habitat for benthic communities in the cove.

Shifts in ascidian taxa associated with habitat stability were reported across several stages of recolonization on a deep shelf floor (>100–270 m) of the Weddell Sea that was impacted by ice scouring (Teixidó et al., 2004). *M. pedunculata* occurred at all successional stages, but was most dominant in the early stage of colonization. On the other hand, *P. setosa* occurred only at the late colonization stage (in the undisturbed assemblage), while *A.* cf. *radiatum* and *Sycozoa sigillinoides* were present in both the relatively stable and undisturbed stages.

In this study, we observed similar patterns in ascidian community shift with the previous studies, although the depth ranges surveyed in the cove were shallower (10–90 m). For example, *M. pedunculata* and *C. verrucosa* were dominant across the entire water depths at sites near the glacier, the most disturbed habitats. On the other hand, *P. setosa* was recorded from 50 to 90 m at MC2, and had its highest density values at 90 m (mean = 4.3 inds·m$^{-2}$), which was apparently the most stable habitat among surveyed areas in this glacial cove. Furthermore, *A.* cf. *radiatum* (at 50 m) and *P.* cf. *discoveri* (70–90 m) were observed only at MC2, and *S. sigillinoides* was found at both MC2 (30 m) and MC3 (50 m), indicating a shift in habitat stability with distance as well as with water depth. Moreover, at MC2, the species composition differed distinctly with water depth and shifts occurred in the dominant species (Fig. 9): *M. pedunculata* and *C. verrucosa* at <30 m; *A. challengeri* at 50–70 m; *A.* cf. *radiatum* and Ascidiacea sp.16 at 50 m; and Ascidiacea sp.17, *P.* cf. *discoveri* and *P. setosa* at 70–90 m. Thus, at the distant site, habitat stability appeared to increase rapidly with depth. The occurrence of abundant large (>20 cm L) hexactinellid sponges (*Anoxycalyx* cf. *joubini* and Rossellidae spp.) at 50–90 m depth in MC2 (Table S1, Fig. 7n) also supported the idea that the habitat at 50–90 m of MC2 was relatively stable and may have been undisturbed for at least several decades (Gutt and Starmans, 2001; Teixidó et al., 2004).

*A. challengeri*, the third most abundant species after *M. pedunculat* and *C. verrucosa* in this cove, occurred across all stations, mostly at >50 m, with the highest abundance (means = 53 inds·m$^{-2}$ and 2 kg·m$^{-2}$) at 50 m in MC2. This finding suggested that *A. challengeri* is more sensitive

to disturbance than *M. pedunculata* or *C. verrucosa*. Unlike *M. pedunculata* and *C. verrucosa* with inflated and erect bodies, *A. challengeri*, is laterally flattened and lie in most cases on the seabed with their siphonal openings near the sediment–water interface, where turbidity is very high due to frequent resuspension of sediment, as compared to the water column above. This difference could explain why *A. challengeri* occurred more abundantly in deeper waters, as turbidity likely decreases with increasing water depth. Its occurrence at all stations, on the one hand, indicates that *A. challengeri* is more tolerant to disturbance than taxa occurring only in deep waters at MC2.

Altogether, sediment properties showed that the deep seabed is physically stabilized toward the outer cove, which contributed strongly to the marked shifts in ascidian assemblages observed across the cove. BIOENV analysis also revealed that ascidian assemblages were strongly related to sediment organic contents, which increased significantly toward the outer cove, suggesting that food availability also contribute, in part, to the observed shifts of ascidian communities in the deep seabed.

## 5. Conclusions

The first ROV survey in Marian Cove, a rapidly warming fjord in WAP, revealed that ascidian community represents epibenthic communities in aspects of abundance, taxonomic diversity and spatial distribution pattern. A set of analyses indicated that ascidian communities shifted drastically in abundance, species composition, and diversity with the longitudinal distance (~3.5 km) across the cove. In particular, such benthic community shift in deep seafloor areas (50–90 m) clearly indicated early colonizing communities near glaciers to more diverse communities at a distant site. The ascidian community shift was related mostly to sediment properties that develop in association with glacial retreat and consequent processes. The sediment properties showed that the deep seabeds are physically stabilized toward the outer cove, which contributed strongly to the marked changes in ascidian assemblages being evidenced across the cove environment.

The results of this study strongly indicated that physical disturbances (sedimentation and ice scouring) accompanying glacial retreat and consequent processes are an important force shaping ascidian assemblages in this cove, and these forces are altered by the distance from the glacier and water depth. In addition to numerical abundance and taxonomic diversity, the differential sensitivity, as reflected by their distributions, of ascidian taxa to habitat perturbation make ascidian communities valuable and sensitive indicators of the impacts of the climate-induced glacial retreat.

Ongoing warming and consequent glacier melting are expected to proceed over the next decade or even longer, particularly in the Antarctic Peninsula Region. Given that distance from the glacier front was roughly proportional to the time of seabed exposure after glacial retreat over the last six decades, the observed ascidian community shift in deep seabed across the cove reflects long-term successional processes that occurred in the past, which in turn provide us an insight into future scenarios for climate-induced changes.

## CRediT authorship contribution statement

**Dong-U Kim:** Conceptualization, Data curation, Formal analysis, Investigation, Methodology, Writing - original draft. **Jong Seong Khim:** Writing - review & editing. **In-Young Ahn:** Conceptualization, Data curation, Investigation, Methodology, Writing - original draft, Supervision, Project administration.

## Declaration of Competing Interest

The authors declare that they have no known competing financial interests or personal relationships that could have appeared to influence the work reported in this paper.

## Appendix A. Supplementary data

Supplementary data to this article can be found online at https://doi.org/10.1016/j.ecolind.2021.107467.

## References

Ahn, I.-Y., Chung, K.H., Choi., H.J., 2004. Influence of glacial runoff on baseline metal accumulation in the Antarctic limpet *Nacella concinna* from King George Island. Mar. Pollut. Bull. 49, 119–127.

Ahn, I.-Y., Moon, H.-W., Jeon, M., Kang., S.-H., 2016. First record of massive blooming of benthic diatoms and their association with megabenthic filter feeders on the shallow seafloor of an Antarctic Fjord: does glacier melting fuel the bloom? Ocean Sci J. 51, 273–279.

Alurralde, G., Torre, L., Schwindt, E., Castilla, J.C., Tatiàn, M., 2013. A re-evaluation of morphological characters of the invasive ascidian *Corella eumyota* reveals two different species at the tip of South America and in the South Shetland Islands, Antarctica. Polar Biol. 36, 957–968.

Anderson, T.J., Cochrane, G.R., Roberts, D.A., Chezar, H., Hatcher., G., 2007. A rapid method to characterize seabed habitats and associated macro-organisms. In: Mapping the Seafloor for Habitat Characterization: Geological Association of Canada Special Paper, pp. 71–79.

Barnes, D.K.A., et al., 2006. Shallow benthic fauna communities of South Georgia Island. Polar Biol. 29, 223–228.

Barnes, D.K.A., Souster, T., 2011. Reduced survival of Antarctic benthos linked to climate-induced iceberg scouring. Nat. Clim. Change 1, 365–368.

Barnes, D.K.A., 2017. Iceberg killing fields limit huge potential for benthic blue carbon in Antarctic shallows. Glob. Change Biol. 23, 2649–2659.

Chang, K.I., Jun, H.K., Park, G.T., Eo., Y.S., 1990. Oceanographic conditions of Maxwell Bay, King George Island, Antarctica (austral summer 1989). Korean J. Polar Res. 1, 27–46.

Cook, A.J., Vaughan, D.G., Luckman, A.J., Murray., T., 2014. A new Antarctic Peninsula glacier basin inventory and observed area changes since the 1940s. Antarct. Sci. 26, 614–624.

Danis, B., 2013. A field guide to Antarctic sponges. Project implemented by SCAR-MarBIN and ANTABIF, Available online at <http://afg.scarmarbin.be/guides/144164-a-field-guide-to-antarctic-sponges>.

Dorschel, B., Gutt, J., Piepenburg, D., Schröder, M., Arndt., J.E., 2014. The influence of the geomorphological and sedimentological settings on the distribution of epibenthic assemblages on a flat topped hill on the over-deepened shelf of the western Weddell Sea (Southern Ocean). Biogeosciences 11, 3797–3817.

Gili, J.-M., Coma, R., Orejas, C., López-González, P., Zabala., M., 2001. Are Antarctic suspension-feeding communities different from those elsewhere in the world? Polar Biol. 24, 473–485.

Gili, J.-M., et al., 2006. A unique assemblage of epibenthic sessile suspension feeders with archaic features in the high-Antarctic. Deep Sea Res. Part II Top. Stud. Oceanogr. 53, 1029–1052.

Gutt, J., Starmans., A., 2001. Quantification of iceberg impact and benthic recolonisation patterns in the Weddell Sea (Antarctica). Polar Biol. 24, 615–619.

Ha, S.-Y., Ahn, I.-Y., Moon, H.-W., Choi, B., Shin., K.-H., 2019. Tight trophic association between benthic diatom blooms and shallow-water megabenthic communities in a rapidly deglaciated Antarctic fjord. Estuar. Coast. Shelf Sci. 218, 258–267.

Hibberd, T., 2009. Field identification guide to Heard Island and McDonald Islands benthic invertebrates. Deep Sea Res Part II Top. Stud. Oceanogr. 53, 985–1008.

Hong, S.G., others, 2019. Overwintering report of the antarctic King Sejong Station 31st Overwintering Party. Korea Polar Research Institute Report 2018.

Kowalke, J., Tatián, M., Sahade, R., Arntz., W., 2001. Production and respiration of Antarctic ascidians. Polar Biol. 24, 663–669.

Lagger, C., Servetto, N., Torre, L., Sahade., R., 2017. Benthic colonization in newly ice-free soft-bottom areas in an Antarctic fjord. PLoS ONE 12, e0186756.

Lagger, C., Nime, M., Torre, L., Servetto, N., Tatián, M., Sahade., R., 2018. Climate change, glacier retreat and a new ice-free island offer new insights on Antarctic benthic responses. Ecography 41, 579–591.

Monniot, F., Dettai, A., Eleaume, M., Cruaud, C., Ameziane., N., 2011. Antarctic Ascidians (Tunicata) of the French-Australian survey CEAMARC in Terre Adélie. Zootaxa 2817, 1–54.

Moon, H.-W., Wan Hussin, W.M.R., Kim, H.-C., Ahn, I.-Y., 2015. The impacts of climate change on Antarctic nearshore mega-epifaunal benthic assemblages in a glacial fjord on King George Island: responses and implications. Ecol. Ind. 57, 280–292.

Oliva, M., et al., 2017. Recent regional climate cooling on the Antarctic Peninsula and associated impacts on the cryosphere. Sci. Total Environ. 580, 210–223.

Peck, L.S., Barnes, D.K.A., Cook, A.J., Fleming, A.H., Clarke, A., 2010. Negative feedback in the cold: ice retreat produces new carbon sinks in Antarctica. Glob. Change Biol. 16, 2614–2623.

Primo, C., Vazquez, E., 2014. Ascidian fauna south of the Sub-Tropical Front. SCAR. pp. 221–228.

Quartino, M.L., Deregibus, D., Campana, G.L., Latorre, G.E., Momo, F.R., 2013. Evidence of macroalgal colonization on newly ice-free areas following glacial retreat in Potter Cove (South Shetland Islands), Antarctica. PLoS One 8, e58223.

Rauschert, M., Arntz, W., 2015. Antarctic Macrobenthos: A Field Guide of the Invertebrates Living at the Antarctic Seafloor. Arntz & Rauschert Selbstverlag.

Rignot, E., Mouginot, J., Scheuchl, B., van den Broeke, M., van Wessem, M.J., Morlighem, M., 2019. Four decades of Antarctic Ice Sheet mass balance from 1979–2017. Proc. Natl. Acad. Sci. USA 116, 1095–1103.

Sahade, R., Tatián, M., Kowalke, J., Kühne, S., Esnal, G., 1998. Benthic faunal associations on soft substrates at Potter Cove, King George Island, Antarctica. Polar Biol. 19, 85–91.

Sahade, R., et al., 2015. Climate change and glacier retreat drive shifts in an Antarctic benthic ecosystem. Sci. Adv. 1, e1500050.

Schories, D., Kohlberg, G., 2016. Marine Wildlife, King George Island. Dirk Schories Publications, Antarctica.

Segelken-Voigt, A., et al., 2016. Spatial distribution patterns of ascidians (Ascidiacea: Tunicata) on the continental shelves off the northern Antarctic Peninsula. Polar Biol. 39, 863–879.

Shin, H.C., others, 2012. Overwintering Report of the 24rd Korea Antarctic Research Program at the King Sejong Station (December 2010-December 2011). Korea Polar Research Institute Report 2011.

Siciński, J., et al., 2011. Admiralty Bay Benthos Diversity—a census of a complex polar ecosystem. Deep Sea Res Part II Top. Stud. Oceanogr. 58, 30–48.

Siciński, J., Pabis, K., Jażdżewski, K., Konopacka, A., Błażewicz-Paszkowycz, M., 2012. Macrozoobenthos of two Antarctic glacial coves: a comparison with non-disturbed bottom areas. Polar Biol. 35, 355–367.

Smale, D.A., Barnes, D.K.A., 2008. Likely responses of the Antarctic benthos to climate-related changes in physical disturbance during the 21st century, based primarily on evidence from the West Antarctic Peninsula region. Ecography 31, 289–305. https://doi.org/10.1111/j.2008.0906-7590.05456x.

Smale, D.A., Barnes, D.K.A., Fraser, K.P.P., 2007. The influence of ice scour on benthic communities at three contrasting sites at Adelaide Island, Antarctica. Austral Ecol. 32, 878–888.

Smale, D.A., Brown, K.M., Barnes, D.K., Fraser, K.P., Clarke, A., 2008. Ice scour disturbance in Antarctic waters. Science 321, 371.

Tatiàn, M., Sahade, R.J., Doucet, M.E., Esnal, G.B., 1998. Ascidians (Tunicata, Ascidiacea) of Potter Cove, South Shetland Islands, Antarctica. Antarct. Sci. 10, 147–152.

Tatiàn, M., Antacli, J.C., Sahade, R., 2005. Ascidians (Tunicata, Ascidiacea): species distribution along the Scotia Arc. Sci. Mar. 69, 205–214.

Teixidó, N., Garrabou, J., Gutt, J., Arntz, W.E., 2004. Recovery in Antarctic benthos after iceberg disturbance: trends in benthic composition, abundance and growth forms. Mar. Ecol. Prog. Ser. 278, 1–16.

Torre, L., et al., 2012. Respiratory responses of three Antarctic ascidians and a sea pen to increased sediment concentrations. Polar Biol. 35, 1743–1748.

Turner, J., et al., 2016. Absence of 21st century warming on Antarctic Peninsula consistent with natural variability. Nature 535, 411–415.

Yoo, K.-C., Lee, M.K., Yoon, H.I., Lee, Y.I., Kang, C.Y., 2015. Hydrography of Marian Cove, King George Island, West Antarctica: implications for ice-proximal sedimentation during summer. Antarct. Sci. 27, 185–196.

Yoon, H.I., Han, M.W., Park, B.-K., Oh, J.-K., Chang, S.-K., 1997. Glaciomarine sedimentation and palaeo-glacial setting of Maxwell Bay and its tributary embayment, Marian Cove, South Shetland Islands, West Antarctica. Mar. Geol. 140, 265–282.

Yoon, H., Park, B.-K., Domack, E., Kim, Y., 1998. Distribution and dispersal pattern of suspended particulate matter in Maxwell Bay and its tributary, Marian Cove, in the South Shetland Islands, West Antarctica. Mar. Geol. 152, 261–275.